Electronic Supplementary Material (ESI) for Soft Matter.

Supplementary Information

3D self-assembly of cells in packed microgel media

Cameron D. Morley, Jesse Tordoff, Christopher S. O'Bryan, Ron Weiss, Thomas E. Angelini

Supplemental Text

Cell body fluctuations. To investigate how fluctuations in cell shape may influence aggregation, we measure the extent of the longest axis of every isolated object detected in time-lapse confocal fluorescence z-stacks at every point in time, $L(t)$. Stacks are processed as decribed in section 2.5 in the manuscript body. The 'PrincipalAxisLength' measurement within the regionprops3 function in MATLAB is used to determine $L(t)$, returning the length of the longest axis of every object. Particle tracking is perfomed to link the same objects together over time. Since cells don't migrate through the gel, tracking is fairly stratight-forward. When objects merge, the earlier tracks are terminated and a new track is started for the new object. To statistically analyze fluctuations of all individual objects over time, we compute the mean-square-fluctuations of each individual $L(t)$, given by $\Delta L^2(\tau) = \left\langle \left(L(t+\tau) - L(t) \right)^2 \right\rangle_t$, where the angle brackets indicate an average over time, t. To test whether $\Delta L^2(\tau)$ exhibits any dependence on the size of the objects, we analyze scatter plots of $\Delta L^2(\tau)$ versus $\langle L \rangle_t$ at each lag time, τ, where $\langle L \rangle_t$ is the average of $L(t)$ over time for each individual object. At any given lag time, τ, we see no clear length-scale dependence, yet the overall point cloud increases to higher values of ΔL^2 with increasing τ (Fig. S4a). To decide how to analyze the ensemble, we create histograms of ΔL^2 for each lag time, τ. We find these ΔL^2 distributions to be highly asymmetric when binned linearly, but more symmetric when binned logarithmically. We find that the distributions are not well described by log-normal statistics, but the median value of ΔL^2 corresponds well to the peaks in the histograms at each lag time, τ (Fig. S4b). Thus, at each lag time we use the median value of ΔL^2 as the representative

square-fluctuation averaged over the population of *n* objects, $\left\langle \Delta L^2(\tau) \right\rangle_n$. A plot of $\left\langle \Delta L^2(\tau) \right\rangle_n$ versus τ reveals that below τ = 2 h, fluctuations grow like $\tau^{1/2}$, and for t between 2 h and 6 h, fluctuations grow like $\tau^{0.9}$ (Fig S4c). From the square-root of $\left\langle \Delta L^2(\tau) \right\rangle_n$, it can be seen that the representative fluctuation in the extent of any of the objects is about 11 μm over the course of about 6 h. The consequences of this result are discussed in the text.

Supplemental Figures

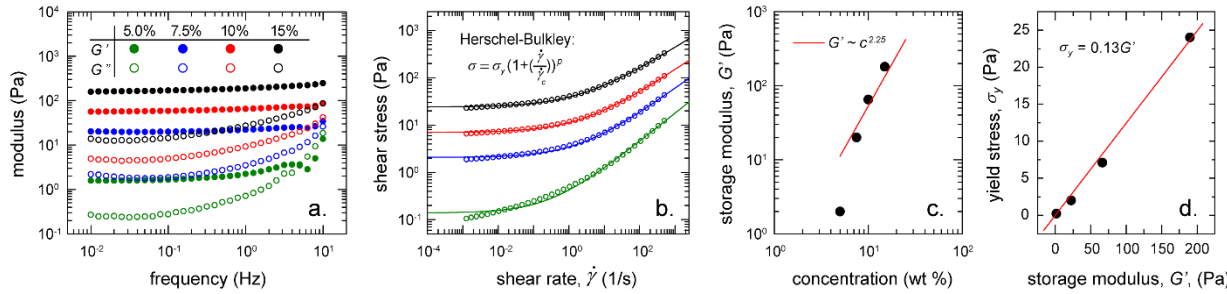

Fig. S1. We conduct rheological characterization of the packed microgel culture media used in our cell aggregation studies. (a) Frequency sweeps at 1% strain amplitude show that the elastic modulus, *G'*, and viscous modulus, *G''* increase with increasing microgel concentration. For most concentrations, *G'* >> *G''* across three decades of frequencies. For the sample at lowest microgel concentration, *G''* begins to dominate *G'* at high frequencies. (b) Unidirectional shear tests exhibit plateaus in shear stress at low shear rates and sub-linear rises in shear stress at high shear rates, as expected of these packed microgel systems. These data are fit to the Herschel-Bulkley model to determine the yield stress. (c) plotting *G*' versus polymer concentration for the packed microgels, we see a sharp increase near the jamming concentration of approximately 4% polymer. At concentrations in the 10-15% range, *G*' raises in a manner consistent with $c^{9/4}$. Such a scaling would suggest that within this concentration range, the pore space between microgels is squeezed out and the jammed system behaves like a continuous gel. (d) Plotting yield stress versus *G'* evaluated at 1 Hz shows the same linear relationship previouisly established in comparable microgel systems.

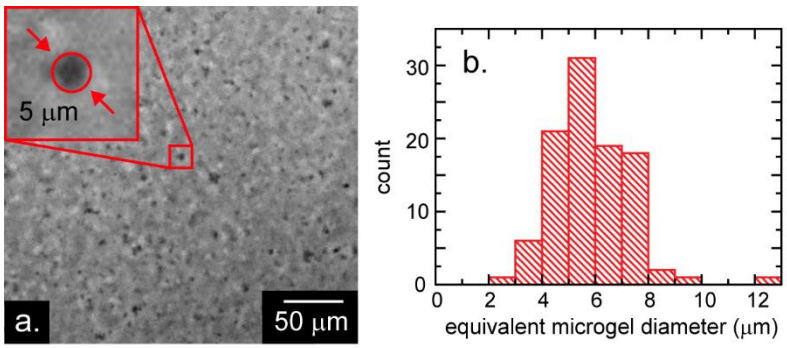

Fig. S2. (a) We examine a diluted sample of microgels under phase contrast microscopy. (b) To determine microgel size, we outline particles from these images and measure their areas using imageJ. Equating these areas to those of equivalent circles, we calculate the equivalent microgel diameter and generate a histogram to find that the average microgel particle is 5 – 6 μm in diameter.

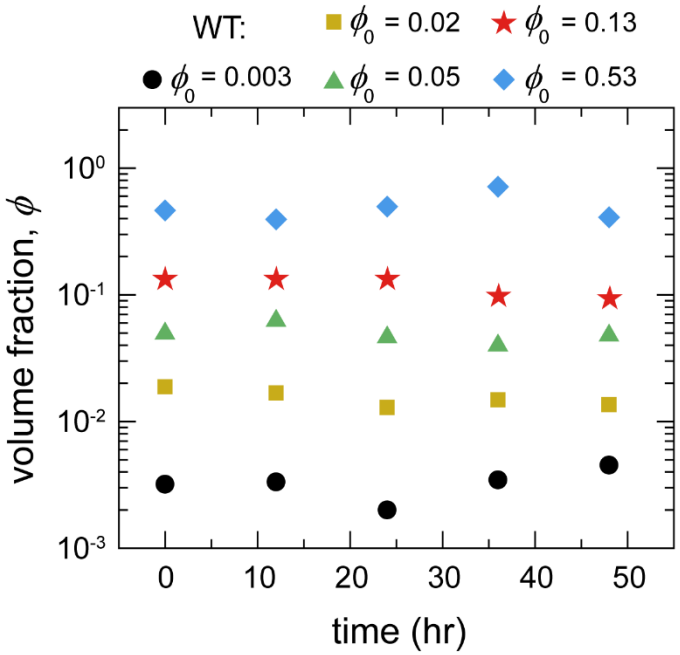

Fig. S3. The average sample volume fraction exhaibits small fluctuations over time relative to the large differences set by the seeding volume fraction. This behavior is consistent with our observing almost no proliferation over the 48 h experiments.

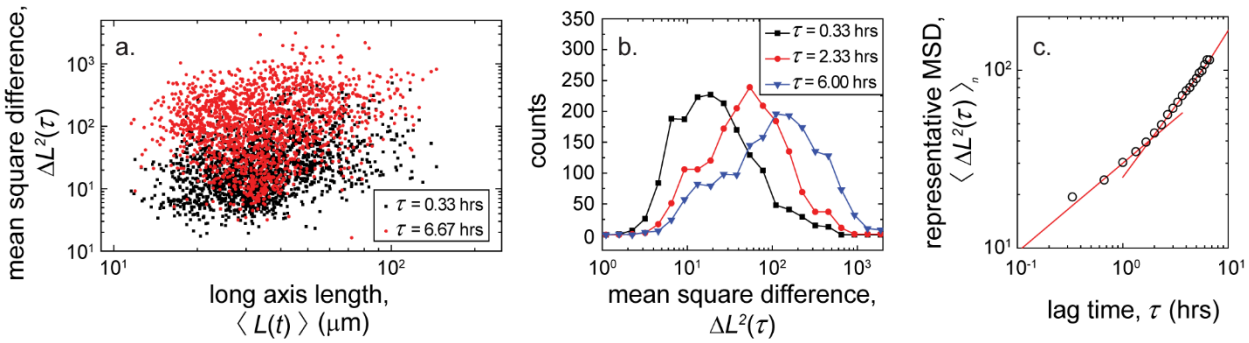

Fig. S4. (a) At any given lag time, τ, we see no clear length-scale dependence of ΔL^2 on L, yet the overall point cloud increases to higher values of ΔL^2 with increasing τ. (b) To choose a represntative ΔL^2 for each t, we perform histogram analysis, finding that the distributions are fairly symmetric when ΔL^2 is sampled logarithmically. We find that the median of ΔL^2 lays close to the peaks in these histograms. (c) Plotting the ensemble-averaged median value of ΔL^2 versus τ, we see that fluctuations in extent of all detected objects exhibit sub-diffusive dynamics. ΔL^2 grows like $\tau^{1/2}$ and short times and like $\tau^{0.9}$ at long times (red lines).

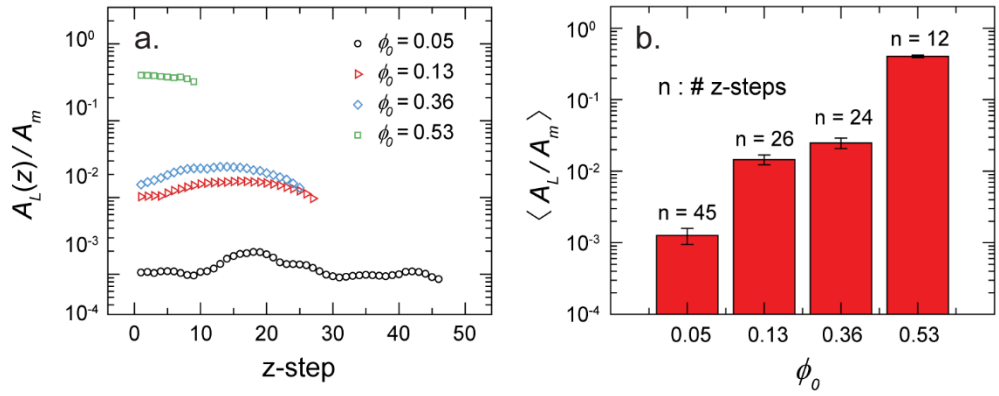

Fig. S5. To test the quality of our imaging as a function of depth into the samples, we examine how A_L / A_m depends on the location along the optical axis of each optical section (z-step). (a) We find that A_L / A_m exhibits no dominating trend as we step into the samples compared to diffferences between samples prepared at different cell volume fractions. We note that we intentionally decrease overall stack thickness with increasing cell density because of light attenuation. (b) Computing the mean and standard deviation of each set of A_L / A_m from (a), we see the relative variations about about the mean decreasing slightly with increasing volume fraction (errorbars denote ± one standard deviation).